Supplementary Information

Mononuclear, hexanuclear and polymeric indium(III) pyrazolido complexes; Structural characterization, dynamic solution studies and luminescent properties

Susana Herrera, Kennett Rivero, Alexis Guzmán, Jonathan Cedeño, Jaroslava Miksovska,* and Raphael G. Raptis.*

Table S1. Selected bond lengths (Å) and angles (°) for complexes **1** - **5**.

	1	**2**	**3**	**4**	**5**
In-Cl	2.47(1)[a]	2.44(1)[a]	2.48(7)[a]	2.48(1)[a]	2.51(1)[a]
	2.45(3)[b]	2.45(5)[b]	2.45(1)[a]	2.46(1)[a]	2.46(3)[b]
	2.48(4)[a]	2.47(5)[a]	2.45(1)[b]	2.45(1)[b]	2.46(1)[a]
In-N	2.26(1)[a]	2.26(1)[a]	2.26(1)[a]	2.26(1)[a]	2.30(1)[a]
	2.30(1)[b]	2.30(3)[b]	2.27(1)[a]	2.27(1)[a]	2.29(1)[b]
	2.26(1)[a]	2.27(1)[a]	2.31(1)[b]	2.32(1)[b]	2.29(3)[a]
N-In-N	84.67(7), 85.76(7)	88.07(8), 90.77(8)	81.8(2), 90.5(2)	81.3(3), 89.4(3)	87.0(1),87.7(1)
	170.36(7)	177.79(8)	172.3(2)	170.6(3)	174.7(2)
Cl-In-N	84.94(5) - 95.99(5)	84.65(5) - 93.50(6)	85.9(2) - 94.4(2)	86.3(2) - 94.8(2)	84.6(1) - 94.2(1)
	176.60(5)	175.17(6)	176.0(2)	175.9(2)	176.2(1)
Cl-In-Cl	95.46(2), 92.15(2)	93.07(3), 95.88(3)	92.14(6), 95.47(6)	92.28(9), 95.10(9)	90.70(5), 91.14(5)
	172.39(2)	170.94(2)	172.28(6)	172.49(9)	176.58(5)

[a]-*trans*-Cl-In-Cl, or *trans*-N-In-N bonds [b]-*trans*-Cl-In-N bonds.

Table S2. Selected bond lengths (Å) for **7 – 9.**

Bond Length (Å)	**7**		**8**	**9**
In···In[a]	3.36(1) – 3.40(4)		3.36(8) – 3.42(9)	3.41(6)
In···In[b]	3.67(2) – 3.74(6)		3.70(4) - 3.73(1)	3.70(5)
In-Cl	2.46(7)	2.48(3)	2.45(4)	2.46(1)
	2.47(6)	2.50(1)	2.46(3)	
	2.48(3)	2.47(4)	2.46(3)	
	2.47(2)	2.48(5)	2.45(2)	
	2.49(2)	2.46(2)	2.45(6)	
	2.48(4)	2.46(1)	2.46(2)	
In-(μ-OH)	2.18(5), 2.19(9)	2.18(8), 2.16(7)	2.20(4), 2.19(7)	2.19(6), 2.20(7)
	2.19(2), 2.19(5)	2.18(5), 2.18(2)	2.18(3), 2.18(6)	
	2.18(4), 2.19(5)	2.18(5), 2.17(7)	2.18(1), 2.18(3)	
	2.19(5), 2.20(6)	2.19(7), 2.18(8)	2.20(3), 2.21(1)	
	2.18(7), 2.20(5)	2.17(6), 2.18(2)	2.18(9), 2.18(7)	
	2.17(6), 2.19(3)	2.20(1), 2.20(7)	2.17(9), 2.18(1)	
In-N	2.20(8), 2.21(4)	2.21(8), 2.21(6)	2.22(5), 2.22(9)	2.21(5), 2.22(1)
	2.20(7), 2.23(7)	2.21(4), 2.21(1)	2.23(5), 2.22(2)	
	2.20(9), 2.21(1)	2.21(6), 2.22(8)	2.22(5), 2.21(7)	
	2.20(2), 2.19(7)	2.20(3), 2.22(4)	2.22(1), 2.22(4)	
	2.21(2), 2.20(8)	2.22(4), 2.22(4)	2.22(1), 2.22(9)	
	2.22(2), 2.21(1)	2.21(1), 2.23(7)	2.21(8), 2.22(1)	
In-(μ_3-$OH_{0.5}$)	2.20(1)	2.20(1)	2.18(1)	2.18(5)
	2.17(3)	2.17(3)	2.19(1)	
	2.20(5)	2.19(9)	2.19(4)	
	2.19(1)	2.16(4)	2.18(2)	
	2.16(9)	2.19(5)	2.19(8)	
	2.18(2)	2.17(3)	2.20(3)	

[a](μ-OH) bridged; [b](μ-pz) bridged.

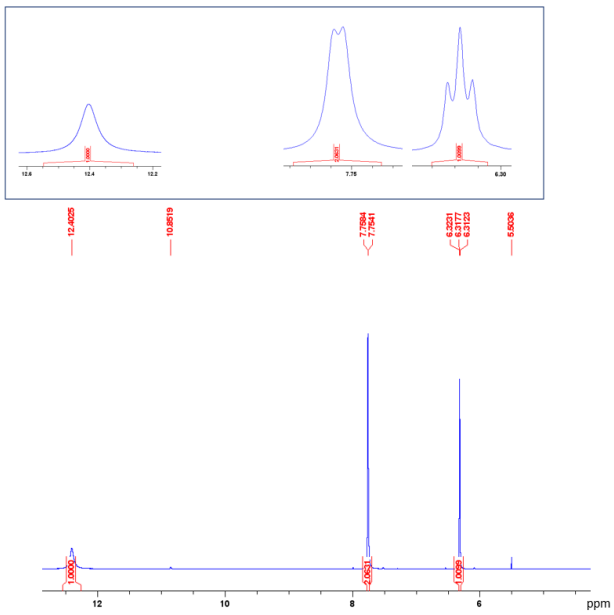

Fig. S2. ^{1}H NMR spectrum of complex **1** in THF-d_8 at RT.

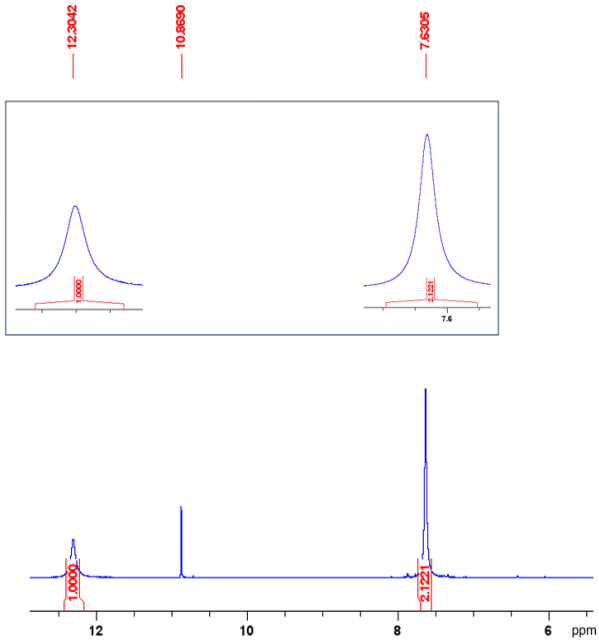

Fig. S3. ^{1}H NMR spectrum of complex **2** in THF-d_8 at RT.

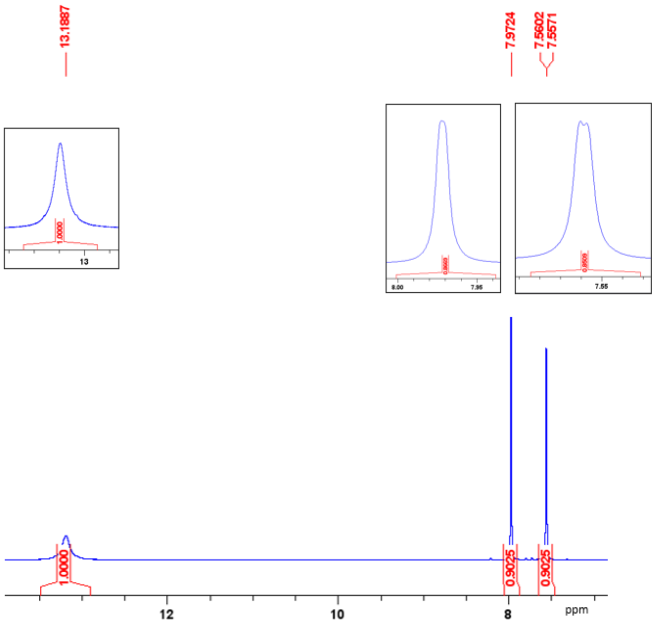

Fig. S4. ^{1}H NMR spectrum of complex **3** in DMSO-d_6 at RT.

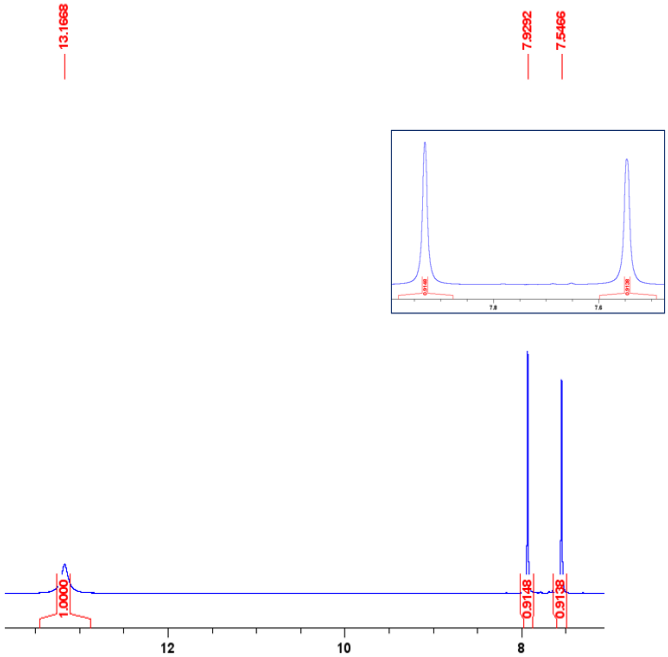

Fig. S5. ^{1}H NMR spectrum of complex **4** in DMSO-d_6 at RT.

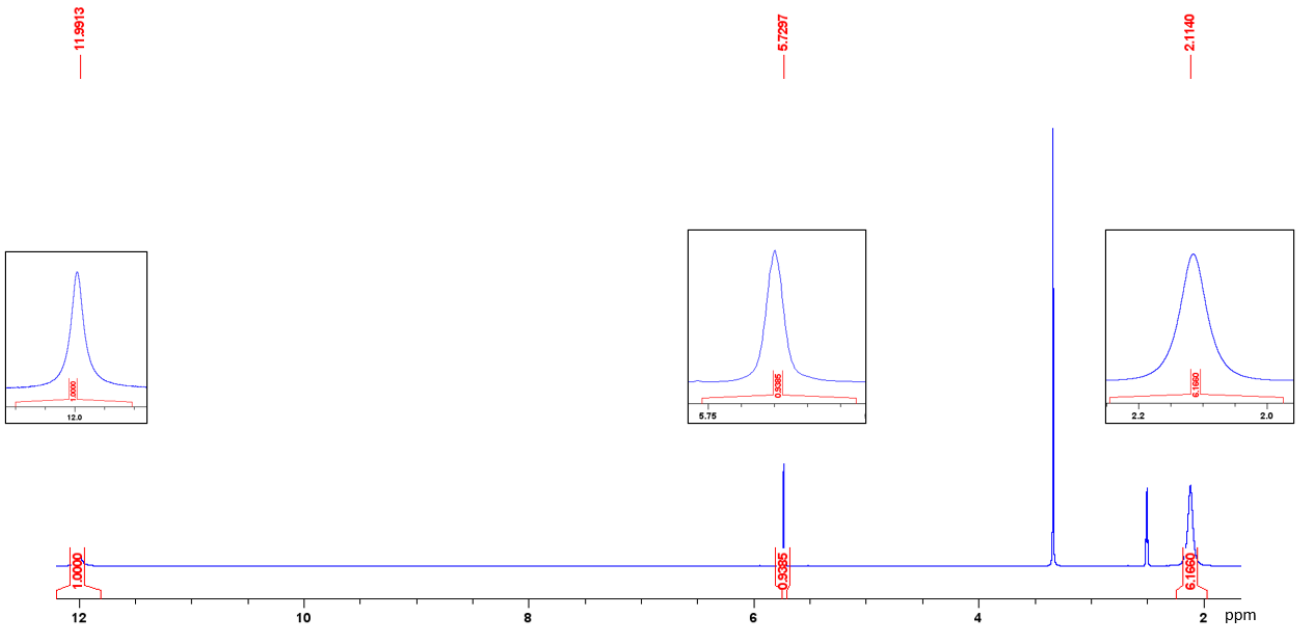

Fig. S6. ^{1}H NMR spectrum of complex **5** in DMSO-d_6 at RT.

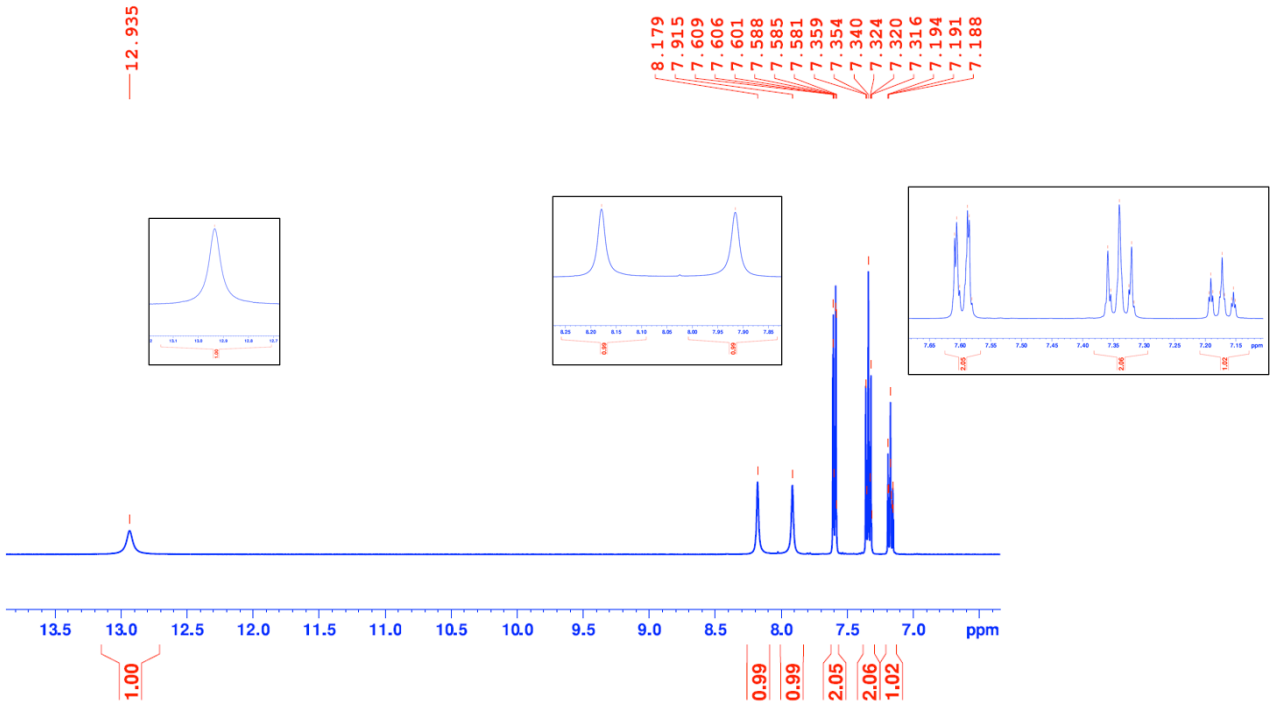

Fig. S7. ^{1}H NMR spectrum of complex **6** in DMSO-d_6 at RT.

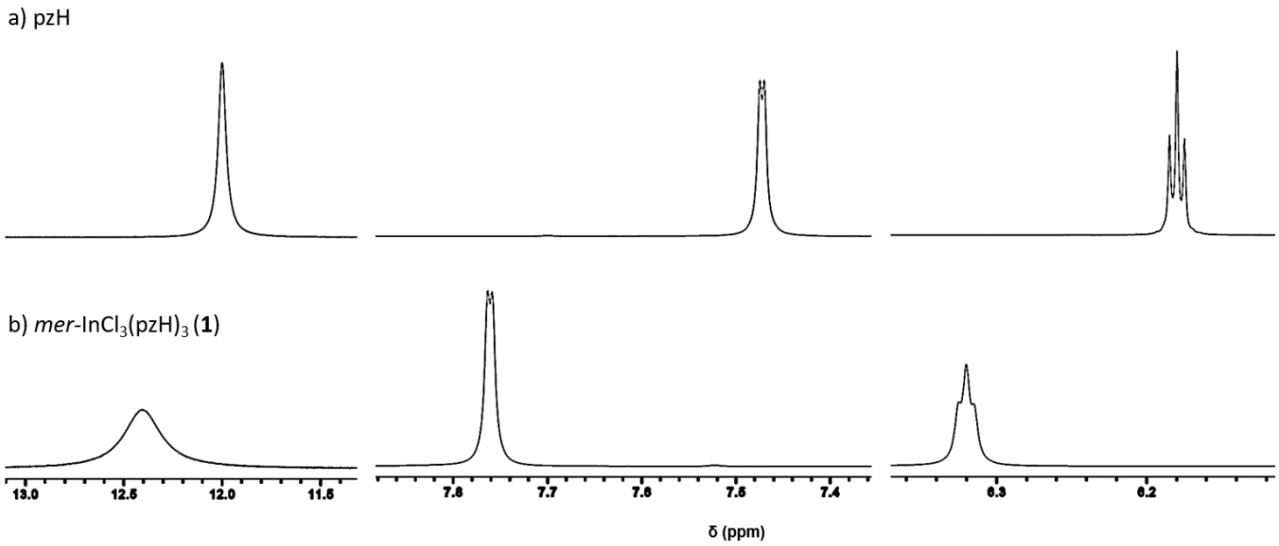

Fig. S8. ^{1}H NMR spectrum of a) pzH in THF-d_8 at RT and b) *mer*-$InCl_3(pzH)_3$ (**1**) in THF-d_8 at RT.

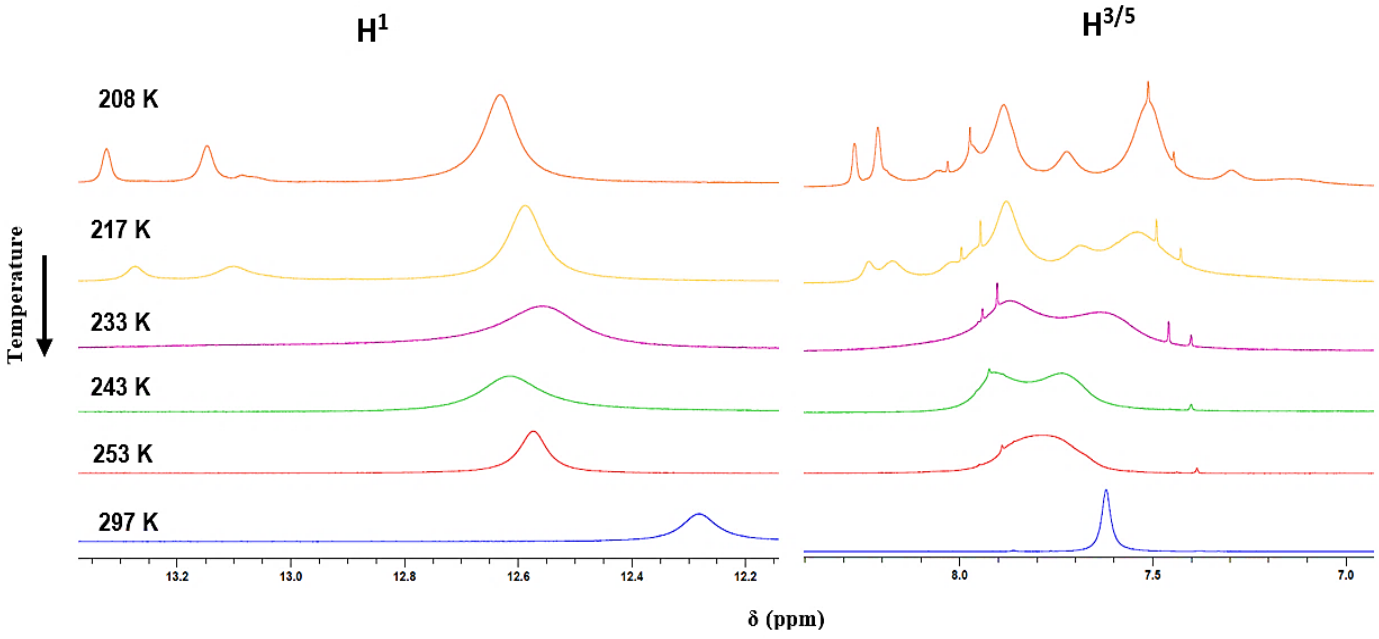

Fig. S9. VT ^{1}H NMR of *mer*-$InCl_3$(4-Cl-pzH)$_3$ (**2**) in THF-d_8, 400 MHz.

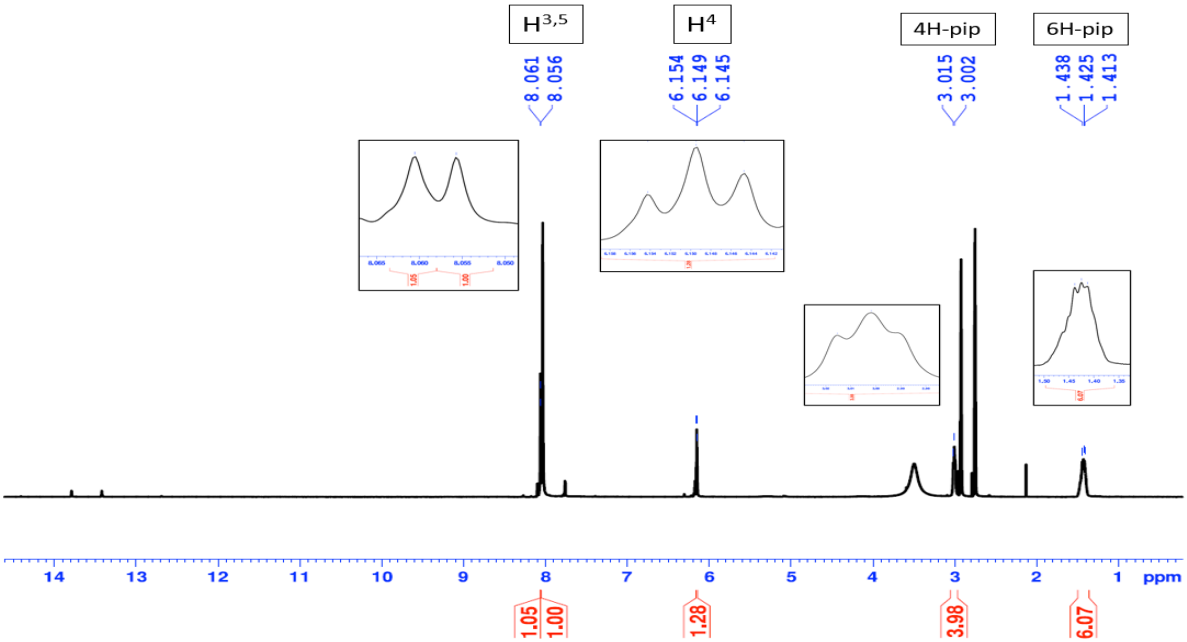

Fig. S10. ^{1}H NMR of $(pipH)_3[In_6Cl_6(\mu_3\text{-}OH_{0.5})_2(\mu\text{-}OH)_6(\mu\text{-}pz)_6]$ (**7**) in DMF-d_7 400 MHz. at RT.

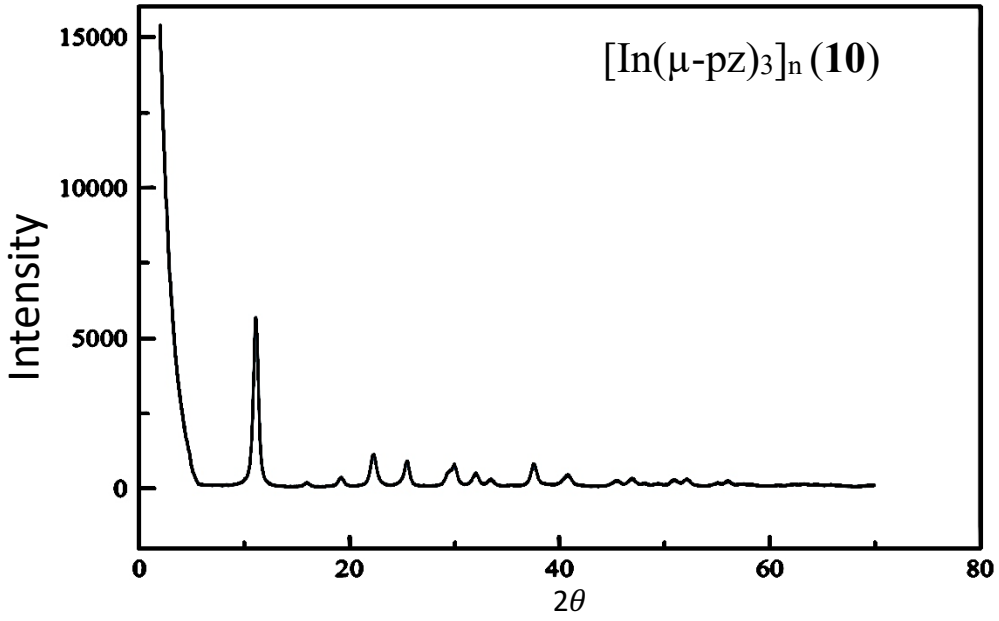

Fig. S11. PXRD pattern for $[In(\mu\text{-}pz)_3]_n$ (**10**).

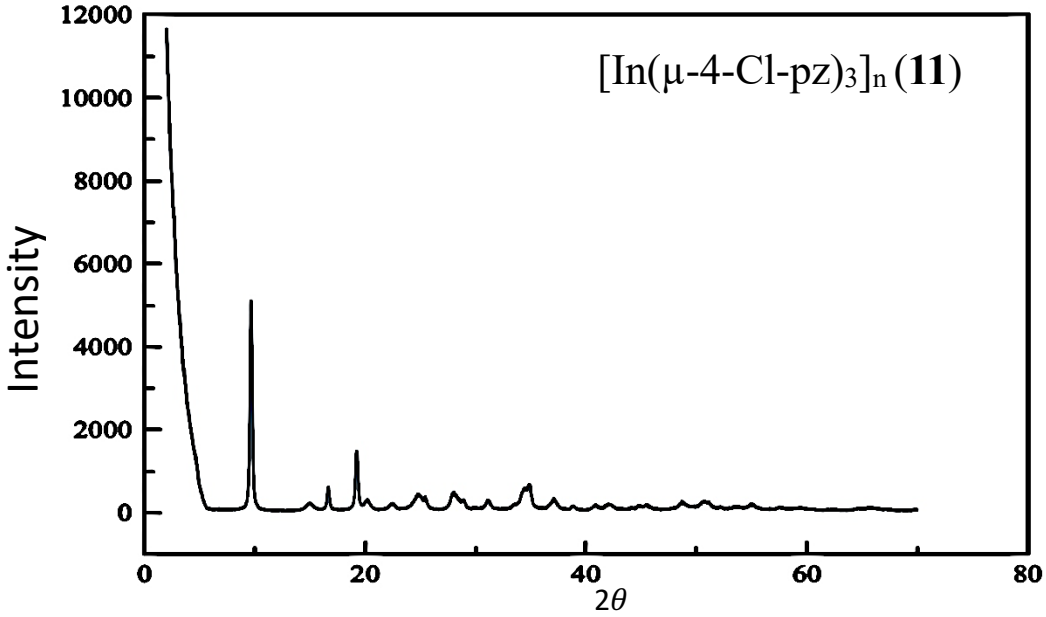

Fig. S12. PXRD pattern for $[In(\mu\text{-}4\text{-}Cl\text{-}pz)_3]_n$ (**11**).

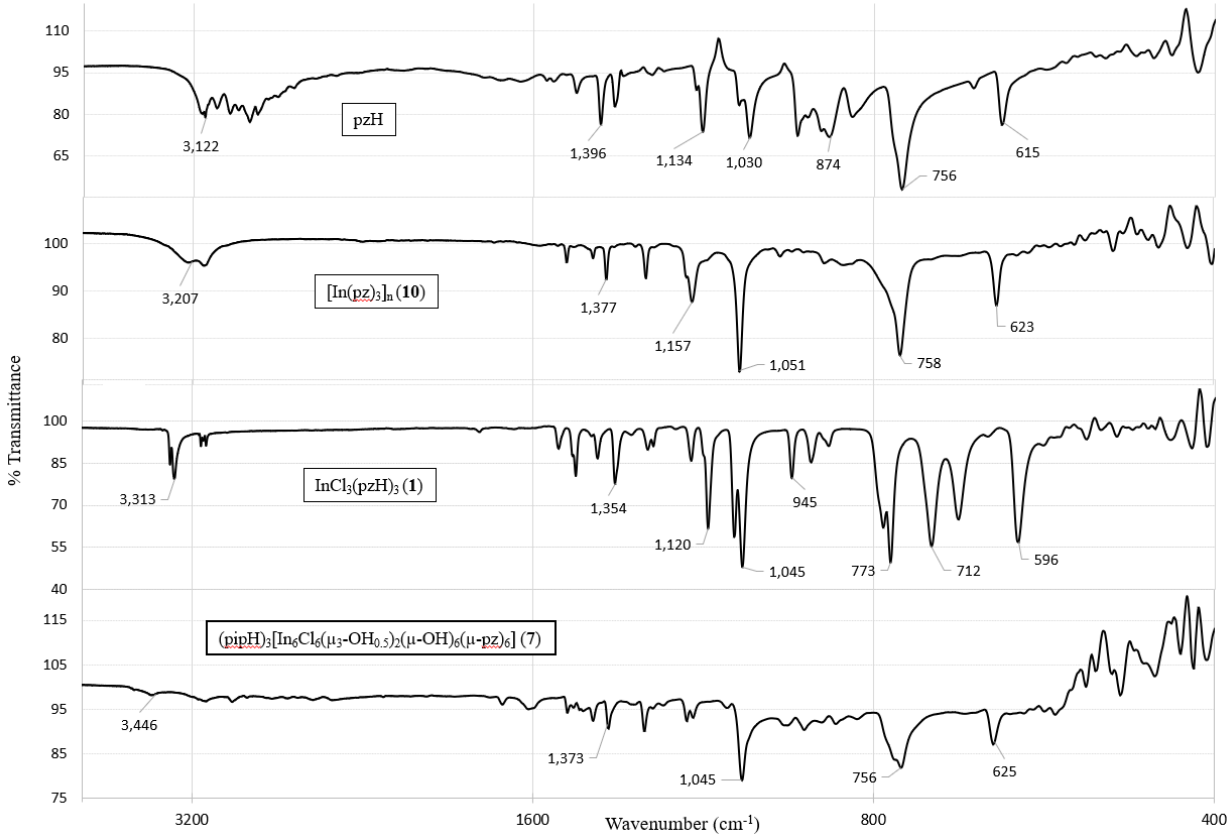

Fig. S13. FT-IR spectra of pzH (top), $[In(\mu\text{-}pz)_3]_n$ (**10**), *mer*-$InCl_3(pzH)_3$ (**1**), $(pipH)_3[In_6Cl_6(\mu_3\text{-}OH_{0.5})_2(\mu\text{-}OH)_6(\mu\text{-}pz)_6]$ (**7**).

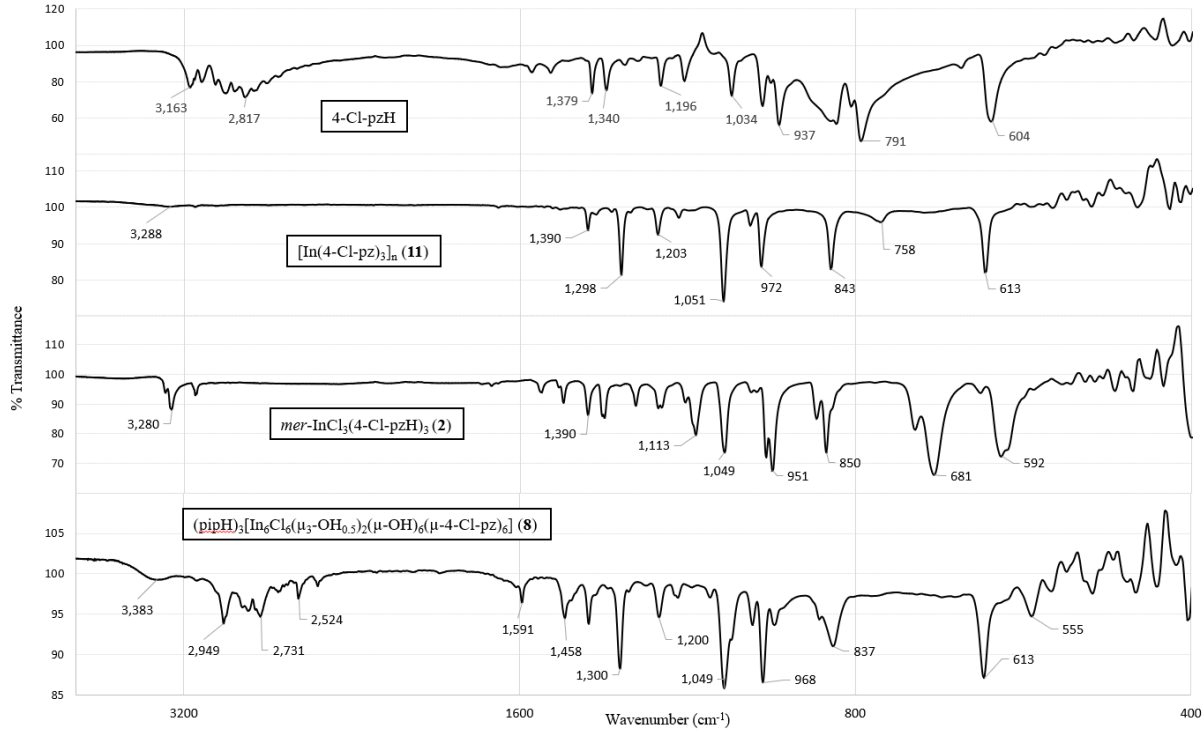

Fig.S14. FT-IR spectra of 4-Cl-pzH (top), $[In(\mu\text{-}4\text{-}Cl\text{-}pz)_3]_n$ (**11**), *mer*-$InCl_3(4\text{-}Cl\text{-}pzH)_3$ (**2**), $(pipH)_3[In_6Cl_6(\mu_3\text{-}OH_{0.5})_2(\mu\text{-}OH)_6(\mu\text{-}4\text{-}Cl\text{-}pz)_6]$ (**8**).

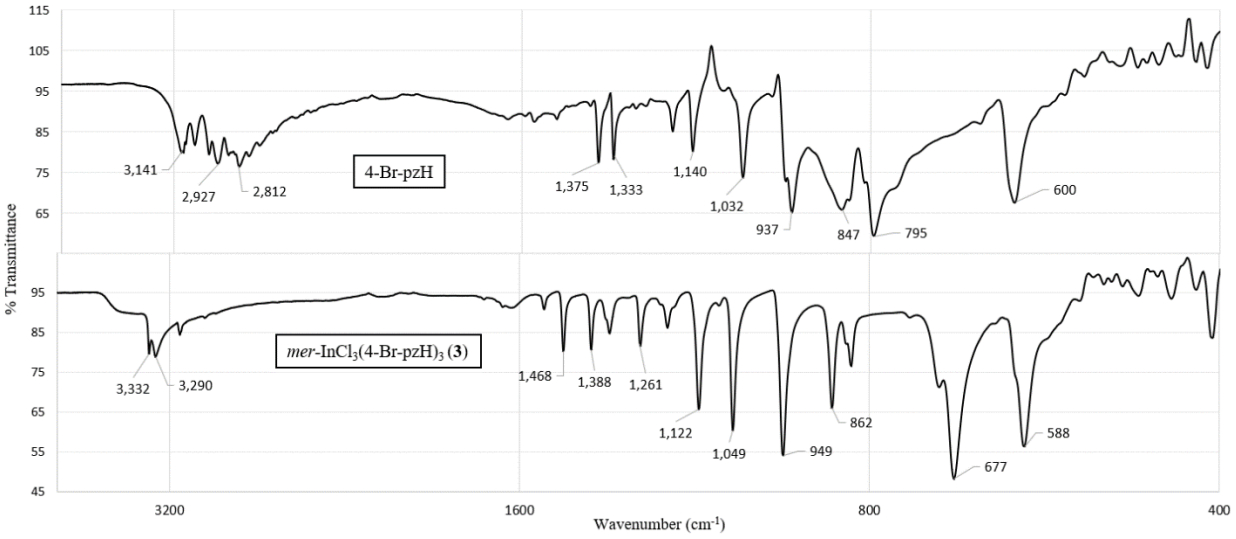

Fig. S15. FT-IR spectra of 4-Br-pzH (top) and *mer*-$InCl_3(4\text{-}Br\text{-}pzH)_3$ (**3**).

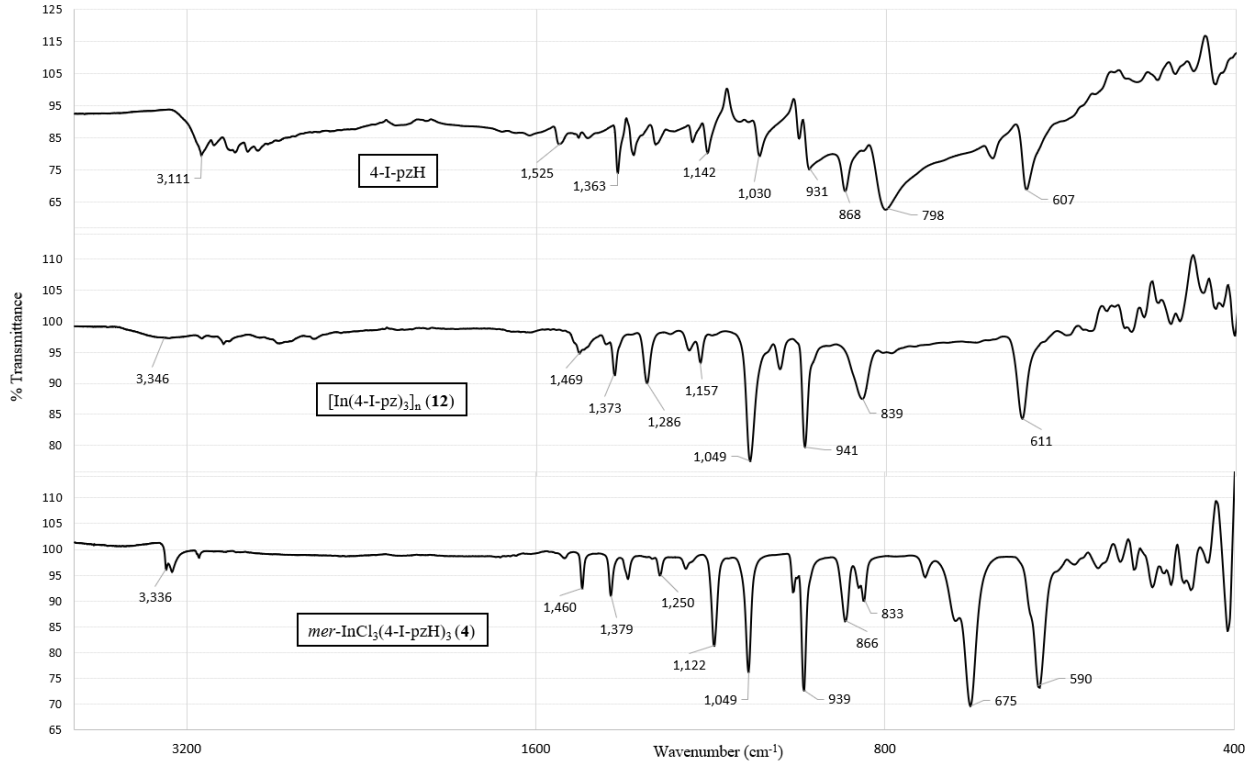

Fig. S16. FT-IR spectra of 4-I-pzH (top), $[In(\mu\text{-}4\text{-}I\text{-}pz)_3]_n$ (**12**), *mer*-$InCl_3(4\text{-}I\text{-}pzH)_3$ (**4**).

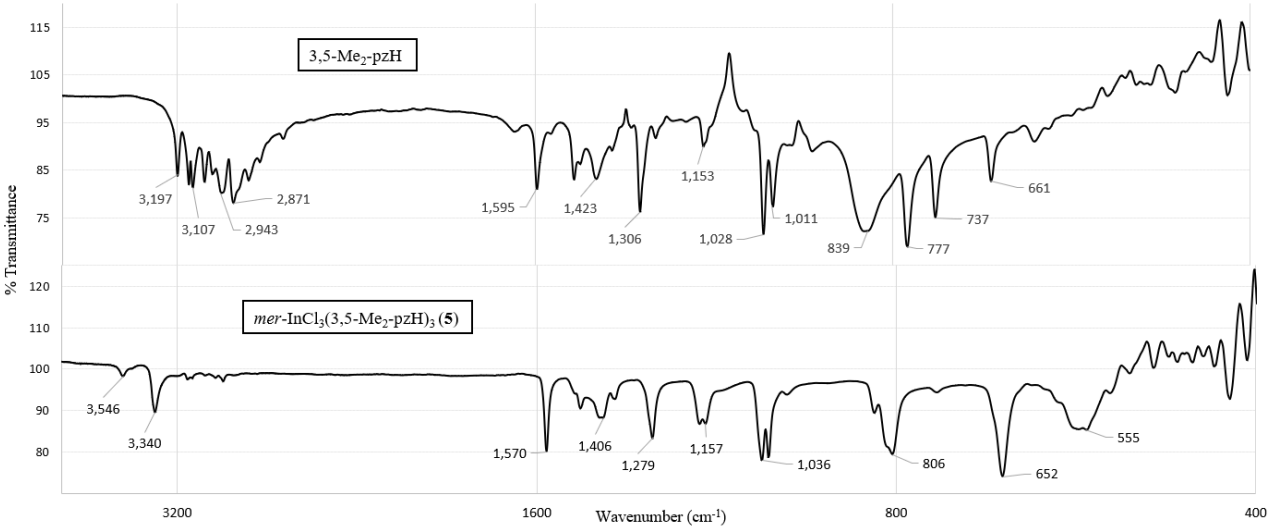

Fig. S17. FT-IR spectra of 3,5-Me_2-pzH (top) and *mer*-$InCl_3(3,5\text{-}Me_2\text{-}pzH)_3$ (**5**).

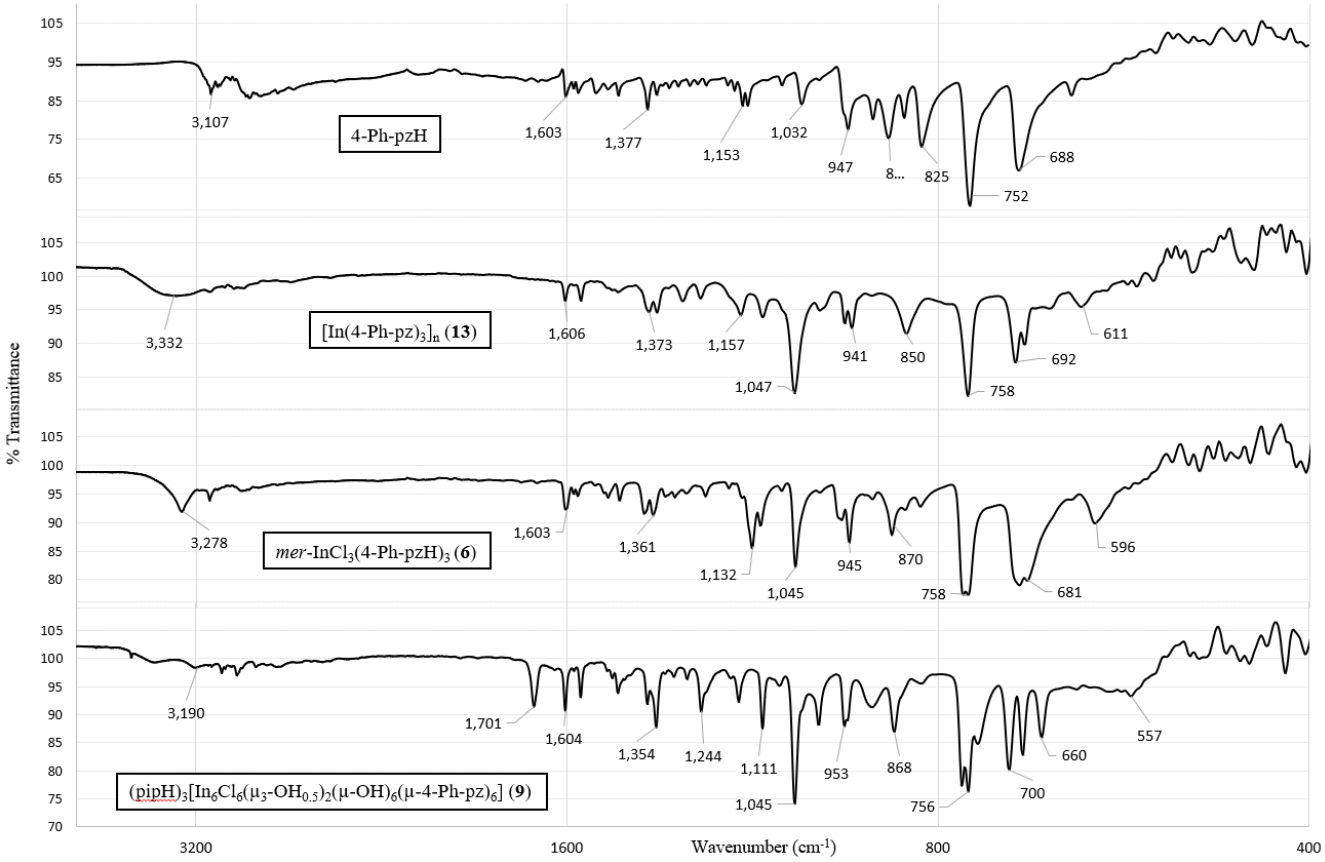

Fig. S18. FT-IR spectra of 4-Ph-pzH (top), $[In(\mu\text{-}4\text{-}Ph\text{-}pz)_3]_n$ (**13**), *mer*-$InCl_3(4\text{-}Ph\text{-}pzH)_3$ (**6**), $(pipH)_3[In_6Cl_6(\mu_3\text{-}OH_{0.5})_2(\mu\text{-}OH)_6(\mu\text{-}4\text{-}Ph\text{-}pz)_6]$ (**9**).

Crystal structures ellipses-and-sticks model

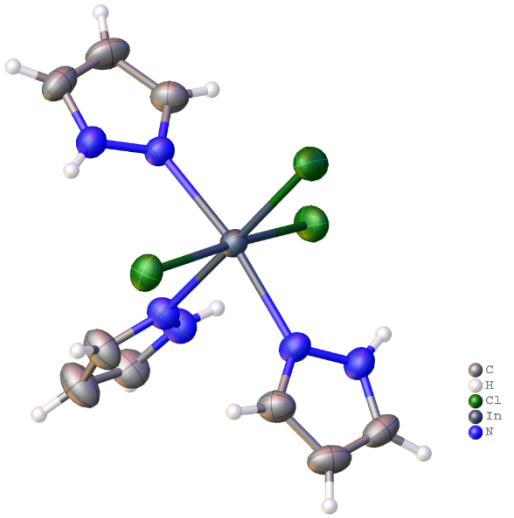

Fig. S19. *mer*-$InCl_3(pzH)_3$ (**1**)

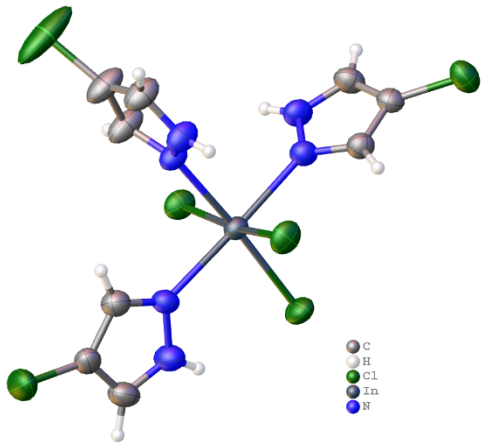

Fig. S20. *mer*-$InCl_3(4\text{-}Cl\text{-}pzH)_3$ (**2**)

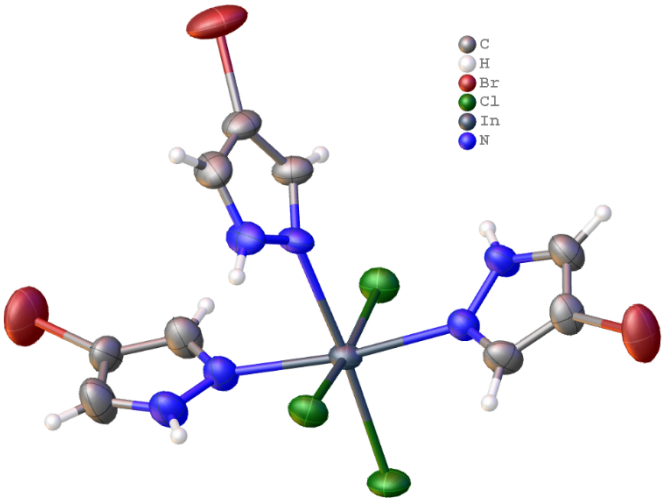

Fig. S21. *mer*-$InCl_3(4\text{-}Br\text{-}pzH)_3$ (**3**)

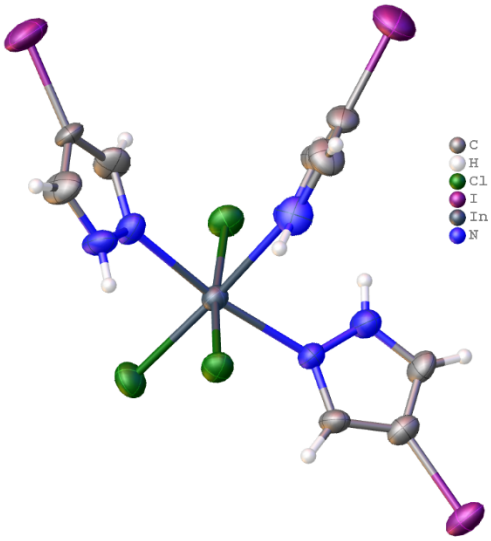

Fig. S22. *mer*-$InCl_3(4\text{-}I\text{-}pzH)_3$ (**4**)

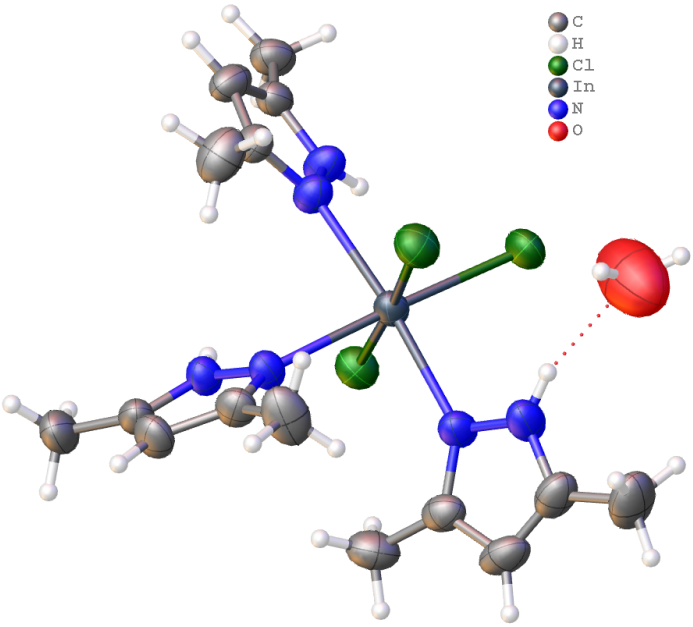

Fig. S23. *mer*-$InCl_3(3,5\text{-}Me_2\text{-}pzH)_3$ (**5**)

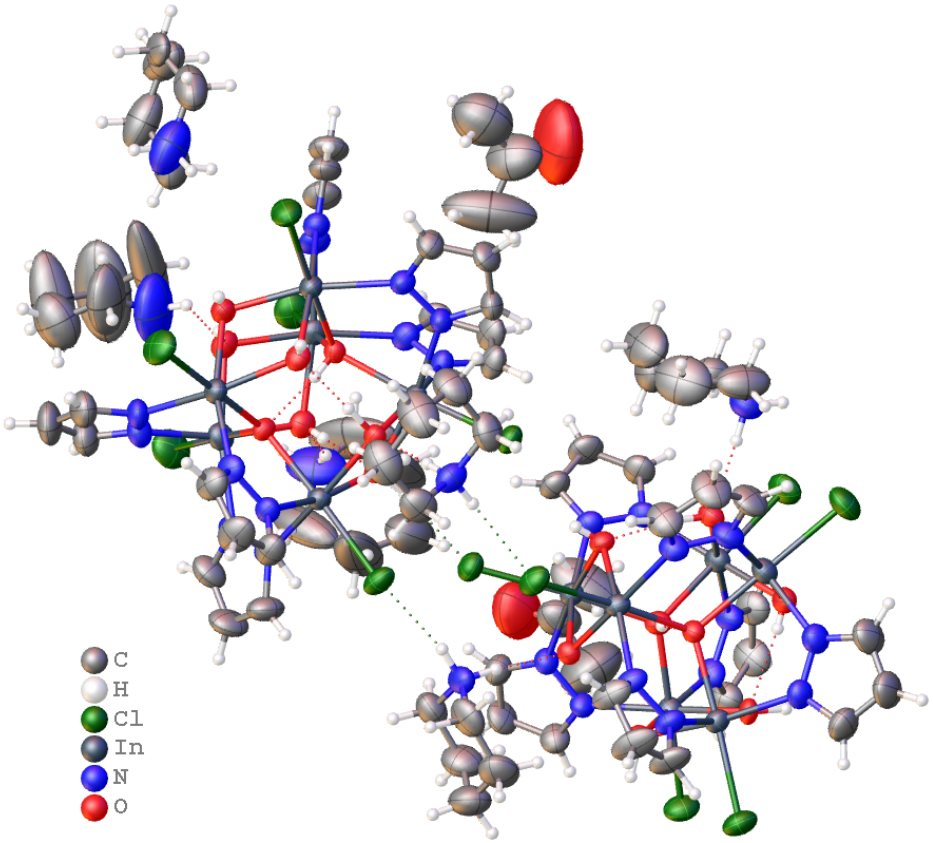

Fig. S24. $(pipH)_3[In_6Cl_6(\mu_3\text{-}OH_{0.5})_2(\mu\text{-}OH)_6(\mu\text{-}pz)_6]$ (**7**)

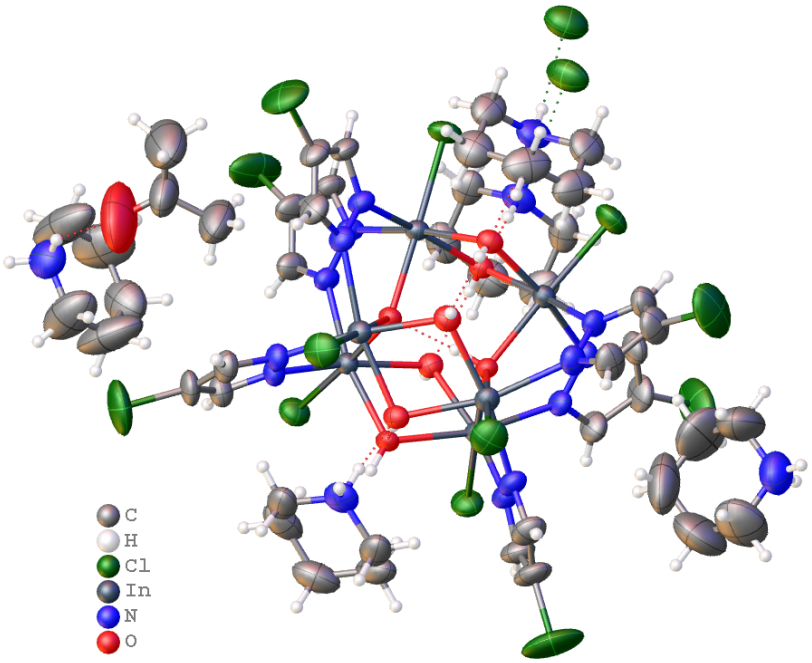

Fig. S25. $(pipH)_3[In_6Cl_6(\mu_3\text{-}OH_{0.5})_2(\mu\text{-}OH)_6(\mu\text{-}4\text{-}Cl\text{-}pz)_6]$ (**8**)

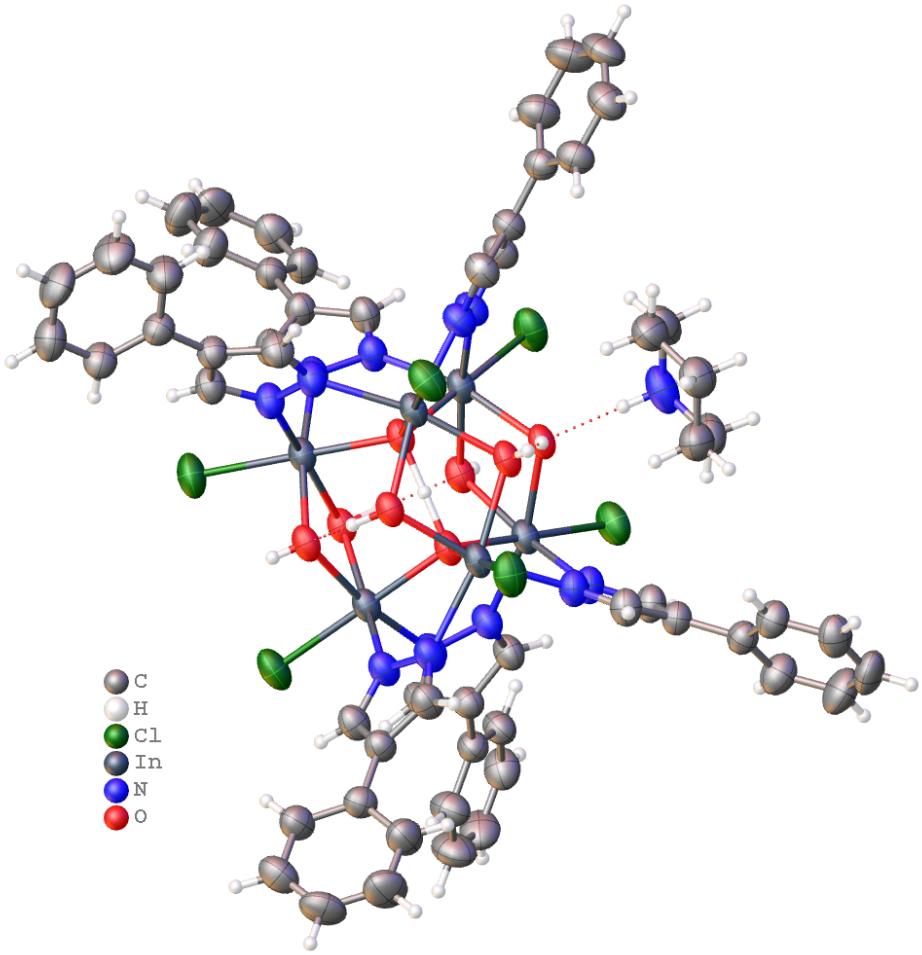

Fig. S26. $(pipH)_3[In_6Cl_6(\mu_3\text{-}OH_{0.5})_2(\mu\text{-}OH)_6(\mu\text{-}4\text{-}Ph\text{-}pz)_6]$ (**9**)